

Ring emission and exciton-pair scattering in semiconductor microcavities

P. G. Savvidis,¹ J. J. Baumberg,^{1,*} D. Porras,² D. M. Whittaker,¹ M. S. Skolnick,³ and J. S. Roberts⁴

¹*Department of Physics & Astronomy, University of Southampton, SO17 1BJ, United Kingdom*

²*Departamento Fisica de Materiales, Universidad Autonoma de Madrid, E-28049, Spain*

³*Department of Physics, University of Sheffield, Sheffield S3 7RH, United Kingdom*

⁴*Department of Electronic and Electrical Engineering, University of Sheffield, Sheffield, S1 3JD, United Kingdom*

(Received 1 October 2001; published 1 February 2002)

Polariton microemitters are semiconductor devices that take advantage of the strong coupling of light and matter to produce efficient optical sources. Injecting an exciton gas into such a semiconductor microcavity can produce annular optical emission of a specific cone angle. We demonstrate that at higher exciton densities or temperatures, this ring continuously decreases in diameter due to the greater energy that can be carried off in exciton-pair scattering processes. These Coulomb-mediated exciton-exciton scatterings are shown to dominate the polariton relaxation and optical emission.

DOI: 10.1103/PhysRevB.65.073309

PACS number(s): 78.45.+h, 32.80.Pj, 42.55.Sa, 71.35.Lk

Semiconductor microcavities are an example of heterostructures in which the coupling of light and matter can be reengineered to produce quasiparticles with highly distorted dispersion relations. The strong coupling of resonant photons in a submicron cavity, with confined excitons embedded in the cavity, creates new physics for optical emission from condensed matter. In planar semiconductor microcavities, an *energy trap* exists for these exciton polaritons, centered around $k=0$ with a narrow momentum width, which is responsible for a number of phenomena. Such a trap differs from the real-space rf and Penning traps used for atomic condensates, but instead functions as a *kinetic* trap in k space, which is fed by dissipation of higher-energy particles.

Much recent interest in this field has been generated by the observation that such polariton systems can show marked nonlinear emission properties when excited by high-energy, nonresonant laser beams.¹⁻³ This interest was further enhanced by recent reports of bosonic stimulated scattering, polariton amplification,⁴⁻⁶ and laserlike oscillation⁷⁻⁹ when the polariton trap was excited resonantly at the point of inflection of its dispersion curve. The macroscopic polariton occupations that result from such stimulated scattering can be harnessed as ultralow threshold emitters, high-gain amplifiers, and as polariton condensates for precision interferometry. However, up to the present time, clear evidence for stimulated scattering and laserlike polariton emission has not yet been reported under *nonresonant* excitation conditions, where excess energy must first be lost before capture into the trap.¹⁰ It is very important to study the mechanisms by which nonresonantly created excitons can drop into an energy trap, since such mechanisms will determine whether *polariton lasers*, free of the restrictions implied by resonant excitation, can be created.

Here we show that the exciton-exciton Coulomb scattering process plays a key role, and that primarily the *shape* of the exciton and polariton dispersions control the relaxation into the trap. A well-defined and cold exciton population is nonresonantly injected into a III-V microcavity in the strong-coupling regime. Strong optical emission is observed in a ring mode, whose angular diameter is determined by the thermal bottleneck condition. As the exciton density is in-

creased, the diameter of the ring mode *continuously decreases*, eventually collapsing to the $k=0$ normal-directed beam. The ring originates from the maximum energy that can be carried off in a two-exciton pair-scattering process.

The strength of pair scattering between excitons has proved hard to measure in semiconductor heterostructures. Semiconductor microcavities are ideally suited for this as the polariton dispersion relation stretches across in-plane wave vectors that can be directly accessed using different angles of incidence.¹¹ However, relaxation of nonresonantly excited excitons into polaritons has variously been attributed to scattering with phonons,^{1,12,13} upper and lower polaritons,^{2,14,15} localized states,^{16,17} and interactions between excitons and exciton or electron-hole pairs.^{3,15,18,19} The question of how polaritons emerge from a population of excitons and how the $k=0$ state is subsequently picked out, is of current debate.

The III-V microcavity sample contains six InGaAs quantum wells (exciton energy $E_x(k) = E_x + [\hbar^2 k^2 / (2M_x)]$, and effective mass M_x) in a $3\lambda/2$ thick spacer between Bragg reflectors, and has been described in detail elsewhere.⁴ The resulting Rabi splitting of the sample, $\Omega = 7$ meV at $T = 10$ K, is sufficient to demonstrate polariton condensation when resonantly pumped at the “magic” angle for energy-momentum-matched polariton scattering ($\theta_m = 16.5^\circ$).^{4,8,9} The modified dispersion relation for the polaritons in the strong-coupling regime forms a polariton trap for lower polaritons of half width at half maximum depth $k_{trap} = \sqrt{6\epsilon\Omega E_x} / \hbar c$ (for a sample effective dielectric constant of ϵ), and of energy depth, $V_{trap} = E_x - E_{LP}(k=0)$ shown in Fig. 1(a). For zero detuning (Δ) between the exciton and cavity mode at normal incidence, this trap depth is equal to half the Rabi splitting, $V_{trap} = \Omega/2$. Under conditions of continuous wave (CW) nonresonant pumping, an exciton-like polariton population (here termed “excitons”) builds up at $k \gg k_{trap}$, which can scatter into polaritons in the trap that are detected by their emission at different angles. A bottleneck in the scattering process has been seen to arise from the steep dispersion near the edge of the trap that retards exciton relaxation.^{3,17} We show here that relaxation of the excitons into the trap is thus critically controlled by the temperature and density of the exciton population.

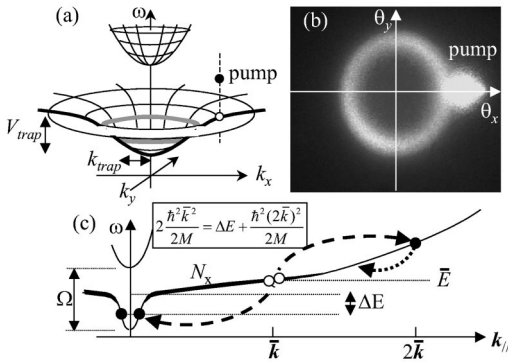


FIG. 1. (a) In-plane 2D dispersion relation of the polariton trap, showing the range of pump energies. (b) Far-field image of the annular output emission for negative detuning $V_{trap} = -15$ meV when pumped at $\theta_p = 30^\circ$, $\Delta_p = 1$ meV, $I_p = 10$ mW, at $T = 10$ K. (c) The exciton-pair scattering process (dashed) producing the maximum energy loss ΔE . The dotted line shows subsequent relaxation of the higher-energy exciton.

Nonresonant injection of excitons is typically achieved by pumping microcavities above the stop band of the Bragg mirrors, providing excess energies more than 100 meV above the band gap. Relaxation of these excitons by optic phonon emission is very fast (~ 100 fs), but further cooling by acoustic emission is much slower. Polariton stability is extremely sensitive to high- k excitons and free e - h pairs, which can ionize polaritons in the trap. To investigate this effect a different pumping scheme is used here to generate a population of excitons. A tunable CW Ti:sapphire laser is focused onto a $50 \mu\text{m}$ spot on the microcavity at angles $\theta > 20^\circ$ ($k_p > k_{trap}$) with photon energies above the lower polariton branch. Although the incoming light cannot couple directly to the polariton branches, the imperfect reflectivity of the top Bragg mirror allows a fraction of the photons through, to be absorbed directly by the quantum wells. Because we find no dependence of our results on either the precise angle of excitation, or on the exact excess energy (pump detuning $\Delta_p = -2$ to $+10$ meV relative to the exciton), this confirms that the excitons absorbed are thermalized. Further evidence for the complete randomization of injected momentum k_p is provided by the observation that all emission is circularly symmetric about the sample normal in this regime, in contrast to previous nonthermal resonantly pumped polariton emission.^{9,20} Light is collected at different angles to the sample normal using a multimode optical fiber in a geometry averaging over $\pm 0.14^\circ$, and analyzed using monochromator and nitrogen-cooled CCD detector. Additionally, far-field images of the emission are recorded using a CCD focused on an image screen placed beyond the sample.

At low excitation powers, in the linear emission regime, most light emerges from the sample in a uniform ring at an angle of 23° for a trap depth, $V_{trap} = -15$ meV [Fig. 1(b)]. This ring directly reveals the bottleneck in the rate of energy relaxation of excitons into the polariton trap. Previously rings have also been seen caused by elastic Rayleigh scattering of the pump^{6,7} but are thus not influenced by energy relaxation. Normalizing by the different emission rate at each

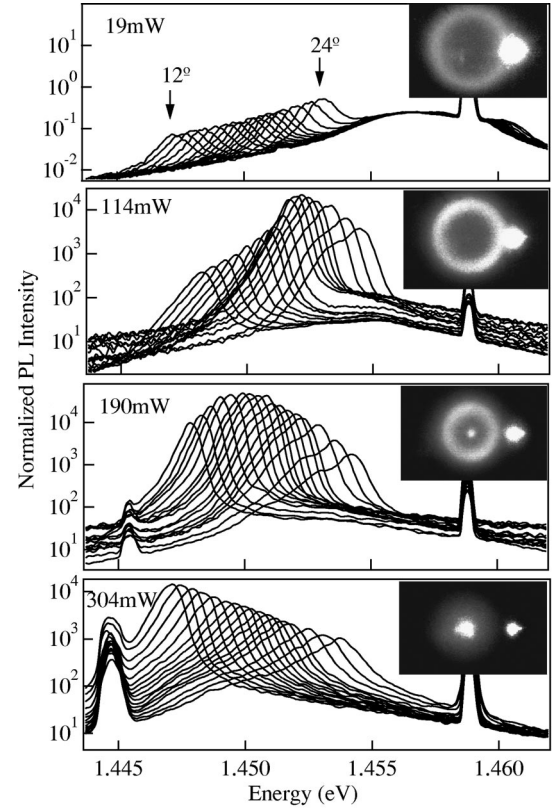


FIG. 2. Photoluminescence spectra at emission angles from 12 – 20° plotted on a log scale, for increasing input pump powers, and normalized by each cavity emission rate. The pump is tuned to 1.459 eV ($\Delta_p = -1$ meV, $\Delta = -15$ meV), $\theta_p = 20^\circ$. Insets: Far-field emission images, showing the transmitted pump at θ_p and the annular emission. The attenuation on the detector is varied to avoid saturation.

angle results in an angular width of the polariton population, $\Delta\theta \sim 5^\circ$. The measured spectral linewidth corresponds to exactly this range of the dispersion relation. In this low-power regime angular emission builds up at the knee of the lower polariton dispersion, always at an energy loss, $\Delta E = E_x - E_{ring} \sim 3$ meV below the exciton energy, irrespective of the cavity detuning conditions. Even for pulsed excitation in this near-resonant excitation geometry we observe similar ring emission behavior.

Above a critical excitation power a regime is observed in which the diameter of the emission ring continuously shrinks (Fig. 2). The angle of maximum emission drops down the dispersion curve together with the photon energy of this emission, while the spectral width at each angle matches the cavity linewidth. Once the angle reaches the magic angle θ_m strong coherent emission at $k=0$ is simultaneously observed [seen as the low-energy peaks in Figs. 2(c) and 2(d)]. This is caused by the polariton-polariton scattering previously identified^{4,9} becoming possible. Above the critical power, the spectral peak at each angle blueshifts by 0.8 meV, as observed previously for parametric scattering and expected from the polariton linewidth,²¹ before slowly red shifting by up to 1 meV ($\ll V_{trap}$) as the power is further increased. The extracted polariton occupation at different points along the

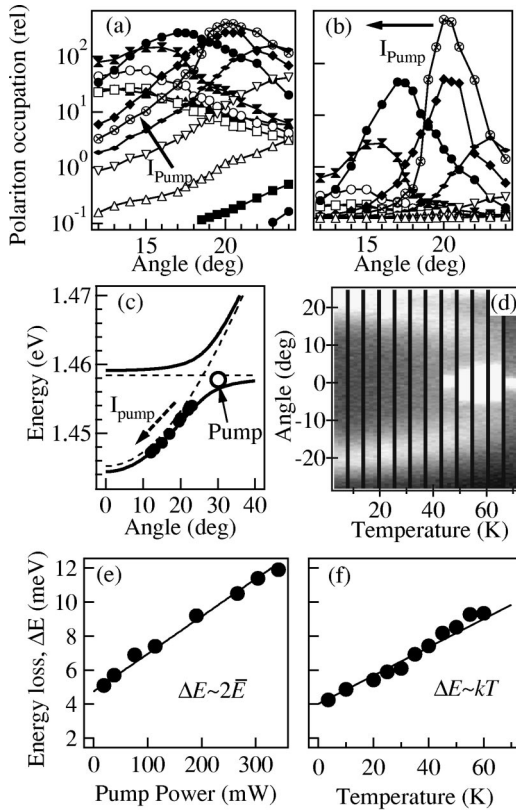


FIG. 3. Angular distribution of polariton occupation (normalized by the pump power) as the pump power at $\theta_p = 30^\circ$ increases from 0.3 mW to 300 mW on (a) log and (b) linear scales. (c) Measured dispersion relation, together with the extracted angles and energies for the ring emission. (d) Equatorial strips of the far-field angular-emission distribution as the temperature increases $I_p = 40$ mW showing onset and collapse of lasing at $k=0$. (e,f) Energy loss ΔE of the dominant polariton emission below that of the exciton, vs (e) pump power and (f) temperature. The solid lines follow the simple theory described in the text.

dispersion curve (normalized by input power) is plotted at increasing pump powers in Fig. 3, and directly shows the strong increase in emission together with the shrinking ring diameter. This behavior contrasts with that for small cavity detunings (producing shallow polariton traps) that show only a broad suppression of polariton occupation below the neck of the trap, that is washed out simultaneously at all k with increasing excitation (where screening leads to collapse of the strong coupling).^{3,18} Here the lack of significant renormalization of the dispersion curves as a function of power [Fig. 3(c)] is due to the small amount of light that tunnels into the cavity to be absorbed as excitons. This is confirmed by direct observation of the persistence of the Rabi splitting between upper and lower polaritons, and also from the lack of emission from the excitonlike upper polariton, showing that the system remains in the strong-coupling regime.

This behavior is evidence of exciton-pair scattering from a thermalized distribution at temperature T . Maximum energy loss is produced by two excitons at average wave vectors \bar{k} mutually scattering via the Coulomb interaction leaving one near $k=0$ and the other at $2\bar{k}$ [Fig. 1(c)]. The energy loss is thus

$$\Delta E = \frac{\hbar^2(2\bar{k})^2}{2M_x} - 2\frac{\hbar^2(\bar{k})^2}{2M_x} = 2\bar{E} = \frac{4\pi\hbar^2}{M_x}N_x,$$

proportional to the incident laser power as found experimentally [Fig. 3(e)]. The fit is obtained with pump-spot diameter $50 \mu\text{m}$, exciton nonradiative lifetime 150 ps, and top mirror transmission $t = 2 \times 10^{-2}$, producing carrier densities $N_x \sim 10^{10} \text{ cm}^{-2}$, below the threshold for exciton saturation. The preference for ring emission is aided by rapid rethermalization of the excitons that end up in high-energy states [Fig. 1(c)]. The previously suggested exciton-pair scattering into an upper and lower polariton¹⁴ is much weaker due to the minimal density of final states in comparison.

Further support for this model is provided by the temperature dependence of the ring emission [Fig. 3(d), $I_p = 40$ mW]. The dispersion relation alters by less than 20% for $T < 70$ K, producing minimal direct effect on the emission. However, as the average wave vector occupied, $\bar{k} = \sqrt{M_x k_B T / \hbar}$ increases, the maximum energy loss, $\Delta E = k_B T$ increases linearly [Fig. 3(f)], matching the observations with no fit parameters. An acoustic phonon model predicts the *opposite* dependence on the lower polariton branch.^{12,15} Detailed microscopic calculations integrating over all possible exciton-exciton scattering processes retain the same qualitative features as presented here, providing strong evidence that polariton relaxation is indeed controlled by scattering of exciton pairs. For $45 \text{ K} < T < 65 \text{ K}$ clear lasing from the bottom of the trap at $k=0$ is observed. However, at higher temperatures we expect the reverse pair scattering process to ionize polaritons out of the trap via high-energy excitons, which indeed prevents lasing for $T > 65$ K. As the cavity detuning is reduced, the polariton trap becomes shallower and it becomes possible for exciton-pair scattering at low temperatures and densities to populate angles below θ_m . Subsequent parametric polariton scattering is then strong, bypassing the regime of ring emission, and yielding lasing at lower temperatures. Thus the buildup of polaritons in the trap is extremely sensitive to occupation at k states beyond $2\bar{k}$, and the depth of the trap.

While the qualitative description from exciton-pair scattering fits the data well, we observe an additional component to the energy loss $\Delta E = 3$ meV, independent of N_x , T , and the microcavity detuning Δ . An initial energy loss can arise from several mechanisms: resonant localized excitons, acoustic phonon emission, or nonthermalized excitons. Localized excitons are present 2.5 meV below the exciton,²⁰ however, their energies do not shift substantially with occupation. The maximum acoustic phonon wave vector emitted by two-dimensional (2D) excitons is determined by the quantum well width L , $k_\perp = 2\pi/L$ providing a maximum theoretical energy loss of 2 meV independent of N_x, T .^{12,15} We also note that this 3-meV energy loss is somewhat universal,^{3,17} and close to half the Rabi splitting. Thus this remaining contribution to the energy relaxation beyond the exciton-pair scattering remains unresolved.

In the simplest picture, *pair* scattering from an incoherent exciton population should present a *quadratic* power dependence. The emission intensity at each angle rises much faster

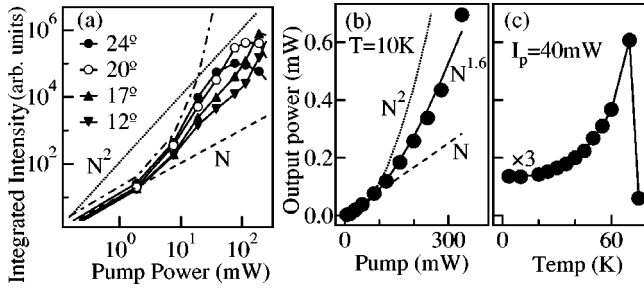


FIG. 4. (a) Intensity emitted at each angle as the pump power increases (same conditions as Fig. 2). Also plotted are linear (dashed), quadratic (dotted), and exponential (dash dotted) dependencies. (b,c) Total output emission collected over angles $|\theta| < \theta_p$, $\theta_p = 30^\circ$ as a function of (b) pump power and (c) temperature.

than this, approaching the exponential enhancement expected from stimulated scattering [Fig. 4(a)]. However, because the ring diameter is simultaneously shrinking, we also measure the total emitted power in the cone $|\theta| < \theta_p$, at a temperature that prevents $k=0$ lasing [Fig. 4(b)]. This also shows a superlinear power dependence ($\propto N_x^{1.6}$) implying more than one particle is involved in the relaxation into polaritons, however, the dependence is now sub-quadratic. These measurements show that power scaling at *specific angles* cannot be used to infer the number of scattering particles.¹⁸ Further evidence for the key role of high- k excitons for pair scattering is found in the strong temperature dependence of the total emission [Fig. 4(c), corresponding to Fig. 3(d)]. Exponentially enhanced thermal population of higher- k states leads to enhanced relaxation into the polariton trap, until for $T > 65$ K ionization out of the trap takes over, drastically curtailing the emission.

Spectral line narrowing is not observed as the ring

shrinks, and the emission at different azimuthal angles around the ring remains incoherent (no interference can be detected between opposite sides of the annulus, and no speckle is observed). Since many azimuthal modes exist for an Airy ring at θ , each mode occupation is too low to reach threshold for lasing. The exception to this is the single $k=0$ mode, which is macroscopically populated when the ring is less than θ_m . This occurs for shallow traps, with small cavity detunings $\Delta > -(\Omega/2)$,³ hence rings are only observed for $\Delta < -(\Omega/2)$. We emphasize the sensitivity of polariton relaxation to occupation of excitons at $\hbar k > \sqrt{M_x \Omega}$ that may account for discrepancies with different methods of exciton production. However, the situation for nonresonant excitation in II–VI microcavities appears qualitatively similar to our observations.¹⁷

In summary, we have observed clear annular emission from semiconductor microcavities pumped with a cold exciton gas. At low-excitation powers, excitons outside the polariton trap scatter into a momentum-space ring due to the bottleneck in relaxation rate. As the temperature or pump power is increased, the largest characteristic exciton momentum increases causing a decrease in the ring diameter, and eventually lasing/condensation at the bottom of the polariton trap. Strong evidence for pair scattering is provided by the agreement of experiment with a simple theory based on the occupation of the quadratic exciton dispersion. Such dynamics is expected to shed light on polariton lasing, leading to improved light emitters.

We are grateful for critical comments from A. I. Tartakovskii, M. Emam-Ismael, C. Weisbuch, J. Bleuse, and D. Le Si Dang and acknowledge the support of HEFCE JR98SOBA, EC CLERMONT HPRN-CT-1999-00132, and EPSRC GR/N18598.

*Electronic mail: j.j.baumberg@soton.ac.uk

¹P. Senellart and J. Bloch, Phys. Rev. Lett. **82**, 1233 (1999).

²D. Le Si Dang *et al.*, Phys. Rev. Lett. **81**, 3920 (1998).

³A.I. Tartakovskii *et al.*, Phys. Rev. B **62**, R2283 (2000).

⁴P.G. Savvidis *et al.*, Phys. Rev. Lett. **84**, 1547 (2000).

⁵G. Dasbach *et al.*, Phys. Rev. B **62**, 13 076 (2000).

⁶J. Erland *et al.*, Phys. Rev. Lett. **86**, 5791 (2001); J. Erland *et al.*, Phys. Status Solidi B **269**, 115 (2000).

⁷R. Houdré, C. Weisbuch, R.P. Stanley, U. Oesterle, and M. Illegems, Phys. Rev. Lett. **85**, 2793 (2000).

⁸R.M. Stevenson *et al.*, Phys. Rev. Lett. **85**, 3680 (2000).

⁹J.J. Baumberg *et al.*, Phys. Rev. B **62**, R16 247 (2000).

¹⁰M. Kira *et al.*, Phys. Rev. Lett. **79**, 5170 (1997).

¹¹G. Khitrova, H.M. Gibbs, M. F. Jahnke, M. Kira, and S.W. Koch, Rev. Mod. Phys. **71**, 1591 (1999).

¹²F. Tassone *et al.*, Phys. Rev. B **56**, 7554 (1997).

¹³J.S. Pau *et al.*, Phys. Rev. B **55**, R1942 (1997).

¹⁴R. Huang, F. Tassone, and Y. Yamamoto, Phys. Rev. B **61**, R7854 (2000).

¹⁵F. Tassone and Y. Yamamoto, Phys. Rev. B **59**, 10 830 (1999).

¹⁶X. Fan *et al.*, Phys. Rev. B **56**, 15 256 (1997).

¹⁷M. Müller, J. Bleuse, and R. Andre, Phys. Rev. B **62**, 16 886 (2000); M. Müller, Ph.D. thesis, Grenoble, 2000.

¹⁸P. Senellart, J. Bloch, B. Sermage, and J.Y. Marzin, Phys. Rev. B **62**, R16 263 (2000).

¹⁹I. Galbraith and S.W. Koch, J. Cryst. Growth **159**, 667 (1996).

²⁰P.G. Savvidis *et al.*, Phys. Rev. B **62**, R13 278 (2000).

²¹C. Ciuti, P. Schwendimann, and A. Quattropani, Phys. Rev. B **62**, R4825 (2000).